Available online at www.sciencedirect.com
ScienceDirect
Journal of Molecular Graphics and Modelling 25 (2006) 487–494
Journal of Molecular Graphics and Modelling
www.elsevier.com/locate/JMGM

A theoretical study of a family of new quinoxaline derivatives

Reinaldo Pis Diez [a], Pablo R. Duchowicz [b,*], Heriberto Castañeta [b], Eduardo A. Castro [b], Francisco M. Fernández [b], Alberto G. Albesa [b]

[a] *CEQUINOR, Centro de Química Inorgánica (CONICET, UNLP), Departamento de Química, Facultad de Ciencias Exactas, Universidad Nacional de La Plata, C.C. 962, 1900 La Plata, Argentina*
[b] *INIFTA, División Química Teórica, Departamento de Química, Facultad de Ciencias Exactas, Universidad Nacional de La Plata, Diag. 113 y 64, Suc. 4, C.C. 16, 1900 La Plata, Argentina*

Received 9 December 2005; received in revised form 12 March 2006; accepted 13 March 2006
Available online 27 March 2006

Abstract

Hybrid density functional calculations are performed on a series of 21 new quinoxaline derivatives, which would likely exhibit important biological activities. Optimized geometries, harmonic vibrational frequencies, and ^{1}H chemical shifts are reported and compared with experimental data when available. In addition, melting points of 75 derivatives are predicted resorting to the Quantitative Structure–Property Relationship (QSPR) Theory, doing the variable selection by means of the Replacement Method and using 875 theoretical descriptors obtained from Dragon 5 software. The best relationship found has seven descriptors with $R = 0.8818$ and $R_{l-10\%-o} = 0.7705$.

Keywords: Quinoxalines; Hybrid density functional theory; Harmonic vibrational frequencies; ^{1}H chemical shifts; QSPR Theory; Multiple regression analysis

1. Introduction

Derivatives of quinoxaline ($C_8H_6N_2$, 1,4-benzodiazine), such as triazolo[4,3-*a*] quinoxaline and quinoxalinecarbonitriles, exhibit excellent bactericidal and fungicidal activities [1,2]. Recently, Moustafa and Abbady reported the synthesis of various quinoxaline derivatives of a new type claiming that they will likely show interesting biological properties [3]. Experimentally, the reaction of 3-ethoxycarbonyl-2-thioquinoxaline (**3**) with active nitriles affords the thiazinoquinoxaline derivatives (**5**–**7**) (see Fig. 1 for reference). Reaction of pyrimidoquinoxalinethione (**9**) with hydrazine hydrate, alkylhalides, phenacyl bromide, and/or bromomalonodinitrile produces compounds (**10**–**13**). The hydrazino compound (**10**) can be used as a starting material to produce other polyheterocyclic systems (**14**–**18**). The authors recorded the IR and ^{1}H NMR spectra of the new species as part of their characterization studies, but no reference to structural parameters is found in that work. In the present work, density functional theory is used to properly characterize the new quinoxaline derivatives obtained by Moustafa and Abbady. Both optimized geometries and harmonic vibrational frequencies and ^{1}H chemical shifts are reported and compared with experimental data when available.

With the purpose of describing further the chemistry of these relatively new compounds, we modeled their melting points (MP) by establishing a Quantitative Structure–Property Relationship (QSPR) model. MP is a common physicochemical property measured when synthesizing new compounds, often used to ascertain purity of organic substances. Its numerical value reflects the magnitude of the intermolecular forces involved in the solid state.

The paper is organized as follows: next section deals with the methodology employed and the computational skills, describing briefly the molecular descriptors calculation in QSPR. After that the results are discussed, while in the final section the general conclusions derived from this study are analyzed.

2. Methodology and computational details

The conformational space of the molecules under study was scanned using the molecular dynamics module of the HyperChem package [4]. The MM+ Molecular Mechanics Force Field available in that package was used for the

* Corresponding author. Tel.: +54 221 425 7430; fax: +54 221 425 4642.
E-mail address: pabloducho@yahoo.com.ar (P.R. Duchowicz).

1093-3263/$ – see front matter © 2006 Elsevier Inc. All rights reserved.
doi:10.1016/j.jmgm.2006.03.004

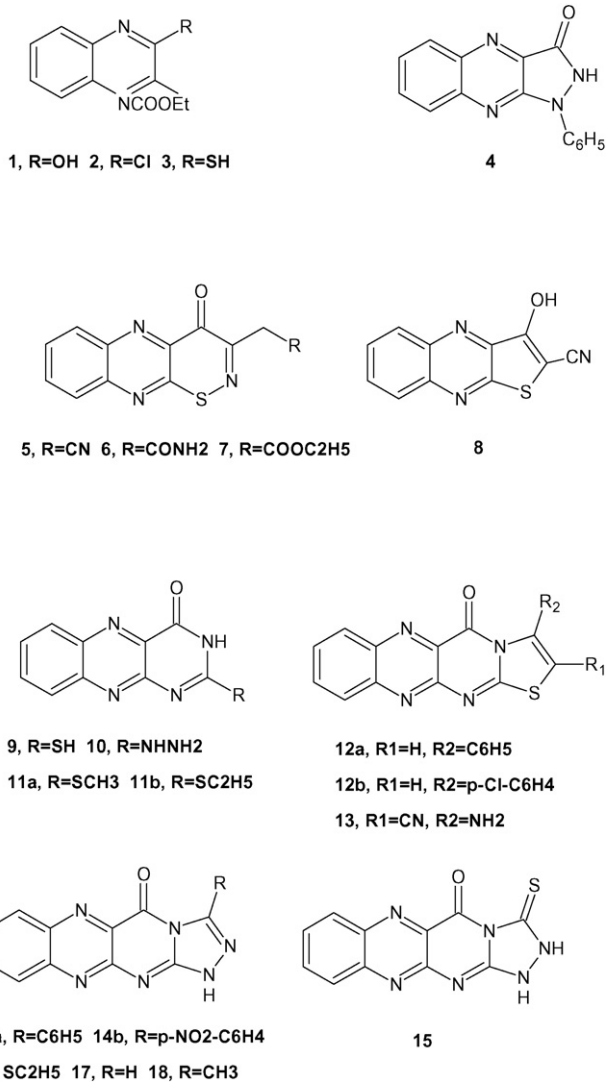

Fig. 1. Schematic drawing of the 21 new quinoxaline derivatives studied in this work.

simulations. The starting geometries were heated from 0 to 900 K in 0.1 ps. Then the temperature was kept constant by coupling the system to a simulated bath with a relaxation time of 0.5 ps. After an equilibration period of about 5 ps, a 500 ps-long simulation was carried out saving the coordinates every 5 ps. The simulation time step was 0.5 fs. The saved geometries were then minimized to an energy gradient smaller than 0.01 kcal mol^{-1} A^{-1} using the MM+ force field.

The lowest-energy conformers found after the above simulations were subjected to further geometry optimizations using the density functional theory [5,6]. To this end, the B3LYP hybrid exchange-correlation functional [7,8] together with the 6-31G(d,p) basis set as implemented in the Gaussian 98 package [9] was used. All geometrical parameters were optimized without constraints.

The harmonic vibrational frequencies were then obtained for the optimized geometry of all the molecules under study in the present work. The frequencies were calculated at the B3LYP/6-31G(d,p) level of theory. The importance of the vibrational

Table 1
Selected optimized dihedral angles (°), obtained for molecules **1–18** at the B3LYP/6-31G(d,p) level of theory

Molecule	Dihedral angle	Value
1	N–C–C–O	−177
	N–C–O–H	0.4
	N–C–C–C	−176.2
	C–C–C–O	32.7
	C–C–C–O	−148.1
	C–C–O–C	−176.7
	C–O–C–C	85
2	N–C–C–C	−175.2
	C–C–C–O	47.1
	C–C–C–O	−134.4
	C–C–O–C	−176.3
	C–O–C–C	85.1
3	N–C–C–C	180
	N–C–C–S	180
	N–C–S–H	0
	C–C–C–O	0
	C–C–C–O	−179
	C–C–O–C	179.7
	C–O–C–C	−84.5
4	N–N–C–C	−169.5
	C–N–N–H	−145.2
5	S–N–C–C	180
	N–C–C–C	0
	C–C–C–N	−177.1
6	S–N–C–C	180
	N–C–C–C	−55.7
	C–C–C–N	53.5
	C–C–C–O	−130.4
7	S–N–C–C	−179.2
	N–C–C–C	113.4
	C–C–C–O	−19.5
	C–C–C–O	162.3
	C–C–O–C	179.5
	O–C–O–C	1.4
	C–O–C–C	85.7
8	C–C–O–H	180
	C–C–C–C	180
	C–C–C–N	174.8
9	N–C–S–H	180
10	C–N–C–N	−177.8
	N–C–N–N	−14.7
11a	C–N–C–S	180
	N–C–S–C	180
11b	C–N–C–S	179.2
	N–C–S–C	177.4
	C–S–C–C	−80.9
12a	N–C–C–C	133.2
12b	N–C–C–C	133.6
13	C–C–N–H	0.3
	N–C–C–C	180
	C–C–C–N	0
14a	N–C–C–C	−147
14b	N–C–C–C	149.1
16	N–N–C–S	179.2
	N–C–S–C	1.4
	C–S–C–C	78.3
18	N–C–C–H	0

Table 2
Experimental, B3LYP/6-31G(d,p), and scaled B3LYP/6-31G(d,p) vibrational frequencies of CO (cm^{-1}), in molecules **1–18**

Molecule	Experimental[a]	B3LYP/6-31G(d,p)[b]	Scaled B3LYP/6-31G(d,p)[c]
4	1670	1835	1697
5	1680	1746	1615
6	1700	1754	1622
7	1680	1749	1617
9	–	1822	1685
10	1660	1816	1679
11a	1660	1821	1684
11b	1670	1820	1683
12a	1690	1810	1674
12b	1680	1809	1673
13	1675	1785	1651
14a	1680	1814	1678
14b	1670	1812	1676
15	1690	1841	1703
16	1700	1807	1671
17	1710	1815	1679
18	1700	1808	1672

[a] Values from Ref. [2].
[b] Present work.
[c] Present work but scaled by 0.9248.

analysis is two-fold. Firstly, it allows to characterize a given conformation as a true minimum on the molecular potential energy surface. Secondly, if the conformation is confirmed to be a minimum then the calculated harmonic frequencies are useful in the assignment of the experimental vibrational data.

Finally, the isotropic chemical shifts for hydrogen atoms were also calculated. In this case, the isotropic magnetic shielding tensor was obtained at the B3LYP/6-311+G(2d,p) level of theory using the geometries already obtained at the B3LYP/6-31G(d,p) level, as suggested in a previous study [10]. The reported shifts are relative to tetramethylsilane (TMS). The absolute isotropic shieldings of TMS were also calculated using the B3LYP/6-311+G(2d,p)//B3LYP/6-31G(d,p) model.

During the QSPR study, all the structures were preoptimized by means of the MM+ force field. Since several molecules contained sulfur atoms, final refined molecular structures were obtained using the semiempirical method Parametric Method-3 (PM3). A gradient norm limit of 0.01 kcal/Å was used for geometry optimization. Several types of molecular descriptors were derived, such as constitutional, topological, geometrical, charge, Geometry, Topology and Atoms-Weighted Assembly (GETAWAY), Weighted Holistic Invariant Molecular descriptors (WHIM), etc., using the software Dragon Version 5 available in the Web for evaluation [11]. In addition, three conceptually important quantum-chemical descriptors that were not provided by this software were added to the pool of variables: HOMO and LUMO energies, and HOMO–LUMO gap. The number of descriptors analyzed resulted in 875.

Since the selection of the best subset of descriptors among thousands of them is not trivial, the Replacement Method (RM) was proposed as a valid tool for this purpose [12,13]. In previous publications it was shown that RM is an approximate method requiring a smaller number of linear regressions than the exact (combinatorial) search of variables, and produces close results. The main idea behind RM is that the minimum standard deviation of the model (S) can be approached by judiciously taking into account the relative errors of the coefficients of the least-squares model given by a set of d descriptors $\mathbf{d} = \{X_1, X_2, \ldots, X_d\}$. In other words, the global minimum of $S(\mathbf{d})$ should be found in a subspace of $D!/[d!(D-d)!]$ points $\mathbf{d}$, where D is the total number of descriptors explored.

3. Results and discussion

Table 1 shows selected dihedral angles of molecules **1–18**, whose structures are shown in Fig. 1. The angles listed in the table involve mainly substituent groups attached to base quinoxaline. The overall optimized geometries are not shown to avoid an overcrowded work. The complete coordinates, however, are available as supplementary material; see Table S1. Tables 2–4 show the vibrational frequencies reported by Moustafa and Abbady [3] and the harmonic vibrational frequencies obtained in the present work for the lowest-energy conformations of molecules **1–18**.

Table 3
Experimental, B3LYP/6-31G(d,p), and scaled B3LYP/6-31G(d,p) vibrational frequencies of NH (cm^{-1}), in molecules **1–18**

Molecule	Experimental[a]	B3LYP/6-31G(d,p)[b]	Scaled B3LYP/6-31G(d,p)[c]
4	3220	3581	3312
9	–	3595	3325
10	3430	3571	3303
11a	3180	3592	3322
11b	3380	3591	3321
14a	3220	3694	3416
14b	3250	3689	3412
15	3180	3559	3291
16	3200	3700	3422
17	3190	3695	3417
18	3210	3699	3421

[a] Values from Ref. [2].
[b] Present work.
[c] Present work but scaled by 0.9248.

Table 4
Experimental, B3LYP/6-31G(d,p), and scaled B3LYP/6-31G(d,p) vibrational frequencies of different groups (cm^{-1}), of molecules **1–18**

Group	Molecule	Experimental[a]	B3LYP/6-31G(d,p)[b]	Scaled B3LYP/6-31G(d,p)[c]
NH_2	**6**	3340	3562	3294
	10	3230	3473	3212
	13	3320	3543	3277
CN	**5**	2220	2383	2204
	8	2220	2333	2158
	13	2220	2313	2139
CS	**15**	1230	1258	1163
OH	**8**	3550	3717	3438

[a] Values from Ref. [2].
[b] Present work.
[c] Present work but scaled by 0.9248.

Table 5
B3LYP/6-311 + G(2d,p) ^{1}H isotropic chemical shifts of different groups (ppm), relative to TMS, of molecules **1–18**

Molecule	ArH	CH	CH_2	CH_3
1	8.36–7.77 (4)[a]	–	5.19–3.91 (2)	1.69–0.99 (3)
2	8.38–7.97 (4)	–	5.20–3.94 (2)	1.74–1.04 (3)
3	8.02–7.52 (4)	–	4.83–3.71 (2)	1.45–0.72 (3)
4	8.77–7.10 (9)	–	–	–
	[8.1–7.3]	–	–	–
5	8.38–7.90 (4)	–	3.74 (2)	–
	[8.0–7.3]	–	[4.3]	–
6	8.41–7.84 (4)	–	4.75–3.02 (2)	–
	[7.9–7.4]	–	[4.5]	–
7	8.38–7.78 (4)	–	4.60–3.26 (4)	1.37–0.58 (3)
	[8.0–7.5]	–	[4.6–3.8]	[1.7–1.4]
8	8.27–7.84 (4)	–	–	–
	[8.3–7.5]	–	–	–
9	8.31–7.70 (4)	–	–	–
10	8.53–7.84 (4)	–	–	–
	[8.0–7.4]	–	–	–
11a	8.57–8.00 (4)	–	–	2.97–2.05 (3)
	[7.9–7.4]	–	–	[2.2]
11b	8.56–7.97 (4)	–	4.15–2.65 (2)	1.96–1.12 (3)
	[8.1–7.4]	–	[3.7–3.4]	[1.5–1.2]
12a	8.60–7.58 (9)	6.50 (1)	–	–
	[8.2–7.3]	[9.5]	–	
12b	8.61–7.57 (8)	6.47 (1)	–	–
	[7.8–7.2]	[9.3]	–	–
13	8.62–8.10 (4)	–	–	–
	[8.3–7.7]	–	–	–
14a	8.60–7.67 (9)	–	–	–
	[7.9–7.5]	–	–	–
14b	8.88–8.00 (8)	–	–	–
	[8.0–7.2]	–	–	–
15	8.60–8.03 (4)	–	–	–
	[8.1–7.7]	–	–	–
16	8.54–7.90 (4)	–	3.64–2.62 (2)	1.92–1.23 (3)
	[8.0–7.5]	–	[4.1–3.8]	[1.5–1.2]
17	8.60–7.97 (4)	8.54 (1)	–	–
	[8.2–7.4]	[8.9]	–	–
18	8.60–7.90 (4)	–	–	3.03–2.46 (3)
	8.0–7.5	–	–	[2.4]

Experimental values are given in brackets when available.
[a] Values in parentheses indicate how many hydrogen atoms give rise to the corresponding isotropic chemical shifts.

Table 6
B3LYP/6-311 + G(2d,p) ^{1}H isotropic chemical shifts of different groups (ppm), relative to TMS, of molecules **1–18**

Molecule	NH	NH_2	OH	SH
1	–	–	5.81 (1)[a]	–
2	–	–	–	–
3	–	–	–	4.76
4	6.42 (1)	–	–	–
	[9.5]	–	–	–
5	–	–	–	–
6	–	6.59–4.11 (2)	–	–
7	–	–	–	–
8	–	–	6.62 (1)	–
	–	–	[9.5]	–
9	7.73 (1)	–	–	4.46 (1)
10	9.14–5.53 (2)	3.31–3.23 (2)	–	–
11a	7.94 (1)	–	–	–
	[8.9]	–	–	–
11b	7.89 (1)	–	–	–
	[9.1]	–	–	–
12a	–	–	–	–
12b	–	–	–	–
13	–	9.09–4.87 (2)	–	–
14a	8.59 (1)	–	–	–
	[10.4]	–	–	–
14b	8.75 (1)	–	–	–
	[10.7]	–	–	–
15	6.55–5.85 (2)	–	–	–
	[11.0]	–	–	–
16	8.22 (1)	–	–	–
	[11.3]	–	–	–
17	8.55 (1)	–	–	–
18	8.21 (1)	–	–	–
	[10.8]	–	–	–

Experimental values are given in brackets when available.
[a] Values in parentheses indicate how many hydrogen atoms give rise to the corresponding isotropic chemical shifts.

It can be seen from the tables that, as expected, the calculated frequencies are higher than the experimental ones. A detailed analysis shows that the calculated CO vibrational frequencies present errors as large as 160 cm^{-1} with respect to experimental values. A scale factor of 0.9334 is obtained for this set of frequencies. The maximum error then decreases to about 60 cm^{-1}, which is an acceptable value. The calculated NH frequencies are very poorly described by the method used in the present work. The errors are as large as 500 cm^{-1}. However, the maximum error diminishes up to about 240 cm^{-1} after a scale factor of 0.8928 is applied. The frequencies reported in Table 4 show a behavior similar to that shown by the CO frequencies with a maximum error of about 240 cm^{-1}. In this case, a scale factor of 0.9476 decreases the maximum error to about 60 cm^{-1}. Finally, an overall scale factor of 0.9248 is obtained for data collected in the three tables. Now, the maximum errors for CO, NH, and the groups shown in Table 4 are about 77, 227, and 112 cm^{-1}. These results clearly indicate that the NH group is in general poorly characterized by the calculated vibrational frequencies. An appropriate scale factor, however, can greatly improve the agreement with experimental data, the average error being of about 8%. It is difficult to establish the source of the discrepancies found between experimental and calculated vibrational frequencies, especially in the NH case, without additional calculations. It can be argued, however, that lattice effects present in the experimental

substances play a fundamental role in stabilizing geometries that could not be achieved by the calculations, which are performed ''in vacuo''. That fact could explain the important errors found for some characteristic groups.

Tables 5 and 6 show the calculated and experimental (when available) ^{1}H isotropic chemical shifts. It can be seen from those tables that the relative chemical shifts for hydrogen atoms binding carbon atoms are very well described by the B3LYP/6-311+G(2d,p)//B3LYP/6-31G(d,p) model. On the other hand, the relative chemical shifts of hydrogen atoms bound to nitrogen and oxygen atoms exhibit important deviations in many cases. It is observed that in all cases the calculated values are lower than the experimental ones. Molecules **4**, **8**, **15**, and **16** present the larger errors ranging from about 2.90 to about 4.50 ppm. Those values represent an average error of about 40%.

As Ref. [3] included only 15 MP of quinoxalines, the calibration set was extended to 75 derivatives for establishing the QSPR model by extracting data from different publications containing structurally related quinoxalines [3,14–17]; the compounds appear listed in Table 7. In those cases where the property was reported in an interval of temperatures, the mean value was considered. The validation of the model was performed with the leave-many-out cross-validation technique, and it was considered that leaving 10% of the compounds out from the calibration set (15 molecules), $R_{l-10\%-o}$, was enough to assert the predictability of the model. The number of random exclusion cases of 15 compounds studied here was 100,000.

The total set of 875 molecular descriptors was first analyzed with the RM method. Since RM does not validate the model when searching for the optimal variables in the pool, one should include in D only those variables that would exhibit acceptable predictive ability during the validation step of the final model. A reasonable strategy for this purpose is the removal, from the initial set D, of those descriptors having identical numerical values for most of the compounds of the calibration set. In this way it is expected that the model descriptors will remain linearly independent when removing molecules from the calibration set, and all of them will contribute to the cross-validation parameters. If a descriptor has repeated entries for many molecules, most probably it will become linearly dependent during the cross-validation procedure and thus will not contribute to predict the property. Proceeding this way, the resulting models have better leave-many-out cross-validation parameters. The details of the relationship found are the following:

$$\begin{aligned} \mathrm{MP}[^\circ\mathrm{C}] &= 192.46 - 51.508\,\mathrm{Mor07u} - 17.568\,\mathrm{nHDon} \\ &\quad - 50.137\,\mathrm{X3sol} + 64.810\,\mathrm{Mor07p} \\ &\quad + 9.819\,\mathrm{XMOD} - 33.324\,\mathrm{H\text{-}047} \\ &\quad + 20.071\,\mathrm{C\text{-}024} \\ N = 75, &\quad R = 0.8818, \quad S = 37.374\,^\circ\mathrm{C}, \quad F = 33.482, \\ &\quad R_{loo} = 0.8448, \quad S_{loo} = 40.216\,^\circ\mathrm{C}, \\ &\quad R_{l-10\%-o} = 0.7705, \\ S_{l-10\%-o} &= 48.400\,^\circ\mathrm{C} \end{aligned} \tag{1}$$

and this equation has no outliers with absolute deviation exceeding 3S, but compound **40** (ethyl 3-(*N*-methyl-*N*-phenyl)-sulfamoylthieno[2,3-*b*]quinoxaline-2-carboxylate) exceeds 2S (86.44 °C). As shown by the cross-validations parameters the model has predictive ability, and the predictions are presented in Table 7. If the predicted versus experimental MP is plotted, the data obey a straight line trend as shown by Fig. 2. Fig. 3 is the dispersion (difference between the experimental and predicted values of the property) as a function of the experimental property, a plot revealing that the deviations are randomly distributed and do not follow any kind of pattern. The absence of data clustering suggests that the seven-variable model is reliable.

The seven descriptors involved in Eq. (1) can be classified as follows: (i) two atom-centred fragments—H-047, the number of hydrogen atoms attached to C^1 (sp^3) or C^0 (sp^2), where the superscript represents the formal oxidation number of the carbon atom (sum of formal bond orders with electronegative atoms), and C024, representing R–CH–R, with R being any group linked through carbon; (ii) two 3D-MoRSE—Mor07u and Mor07p, symbolizing signal 07, unweighted and weighted by atomic polarizabilities, respectively; (iii) one functional group—nHDon, the number of donor atoms for H-bonds (with N and O); (iv) two topological indexes—XMOD, a modified definition of the Randic chi-1 index; and X3sol, solvation connectivity index chi-3. The importance of the descriptors in

Table 7
Experimental and predicted MP (°C) for 75 quinoxaline derivatives

n	Compound name	MP experimental	MP predicted	Diff.[a]
1	3H-pyrazolo[3,4-*b*]quinoxalin-3-one, 1,2-dihydro 1-phenyl-	235.5	205.4	30.07
2	4H-1,2-thiazino[5,6-*b*]quinoxaline-3-acetonitrile, 4-oxo-	242	259.3	−17.38
3	4H-1,2-thiazino[5,6-*b*]quinoxaline-3-acetamide, 4-oxo-	255.5	253.7	1.795
4	4H-1,2-thiazino[5,6-*b*]quinoxaline-3-acetic acid, 4-oxo-, ethyl ester	195	244.2	−49.27
5	Benzo[*g*]pteridine-2,4(1H,3H)-dione, 2-hydrazone	285	258.3	26.65
6	Benzo[*g*]pteridin-4(1H)-one, 2-(methylthio)-	168	207.4	−39.47
7	Benzo[*g*]pteridin-4(1H)-one, 2-(ethylthio)-	156	210.3	−54.3
8	5H-benzo[*g*]thiazolo[2,3-*b*]pteridin-5-one, 3-phenyl-	274	229.6	44.3
9	5H-benzo[*g*]thiazolo[2,3-*b*]pteridin-5-one, 3-(4-chlorophenyl)-	248	238.4	9.572
10	5H-benzo[*g*]thiazolo[2,3-*b*]pteridine-2-carbonitrile, 3-amino-5-oxo-	234	247.4	−13.48
11	Benzo[*g*]-1,2,4-triazolo[3,4-*b*]pteridin-5(1H)-one, 3-phenyl-	284	301.8	−17.88

Table 7 (*Continued*)

n	Compound name	MP experimental	MP predicted	Diff.[a]
12	Benzo[*g*]-1,2,4-triazolo[3,4-*b*]pteridin-5(1H)-one, 3-(4-nitrophenyl)-	311	303.2	7.761
13	Benzo[*g*]-1,2,4-triazolo[3,4-*b*]pteridin-5(1H)-one, 2,3-dihydro-3-thioxo-	293	277.3	15.67
14	Benzo[*g*]-1,2,4-triazolo[3,4-*b*]pteridin-5(1H)-one, 3-(ethylthio)-	196.5	224.4	−27.92
15	Benzo[*g*]-1,2,4-triazolo[3,4-*b*]pteridin-5(1H)-one, 3-methyl-	296	298	−2.001
16	3-Ethoxycarbonyl-quinoxalin-2(1H)thione	187	180.5	6.491
17	1,2H-(pyrazolo[4,5-*b*]quinoxaline)-3-one	220.5	233.4	−12.9
18	1,2,3,4-Tetrahydro-4-oxo-pyrimido[4,5-*b*]quinoxalin-2-thione	275	230.9	44.03
19	3-(3′-Mercapto-1′,2′,4′-oxadiazol-5′-yl)quinoxalin-2(1H)-one	290	301.1	−11.11
20	2(1H)-quinoxalinone, 3-[5-(methylthio)-1,3,4-oxadiazol-2-yl]-	175	145.1	29.89
21	2(1H)-quinoxalinone, 3-[5-[(2-oxo-2-phenylethyl)thio]-1,3,4-oxadiazol-2yl]-	164	200.9	−36.91
22	Oxazolo[4,5-*b*]quinoxalin-2(3H)-one	335	286.1	48.88
23	*N*,*N*′[Bis(quinoxalin-2(1H)-one-3-yl)] urea	340	312.7	27.27
24	3-Piperidinocarbonylamino-quinoxalin-2(1H)-one	265	211.7	53.26
25	2-Chloro-3-piperidinocarbonylaminoquinoxaline	140	162.2	−22.29
26	3-Piperidinocarbonylaminoquinoxalin-2(1H)-thione	225	248.9	−23.93
27	2-Hydrazino-3-piperidinocarbonylaminoquinoxaline	285	258.7	26.24
28	3-Methoxycarbonylamino-quinoxalin-2(1H)-one	218	214.1	3.81
29	2(1H)-quinoxalinone, 3-[[5-(methylthio)-1H-1,2,4-triazol-3-yl]amino]-	210	174.5	35.43
30	2(1H)-quinoxalinone, 3-[[5-[(2-oxo-2-phenylethyl)thio]-1H-1,2,4-triazol-3-yl]amino]-	228	243.6	−15.67
31	3-(Amino-3′-hydrazino-1′,2′,4′-triazolo-5′-yl)quinoxalin-2(1H)-one	305	341.7	−36.76
32	3-(Quinoxalin-2(1H)-one-yl)-azo-naphthol	188	227.3	−39.3
33	2(1H)-quinoxalinone, 3-[(phenylmethylene)amino]-	340	302.9	37.07
34	2(1H)-quinoxalinone, 3-[[(4-nitrophenyl)methylene]amino]-	355	364.2	−9.239
35	3-Acetylamino-quinoxalin-2(1H)-one	295	307.4	−12.45
36	2-Methyl-oxazolo[4,5-*b*]quinoxaline	325	286.1	38.88
37	3-Amino-2-ethoxycarbonylthieno[2,3-*b*]quinoxaline	145	127	17.9
38	2-Ethoxycarbonylthieno[2,3-*b*]quinoxaline-3-diazonium chloride	258	218.7	39.25
39	2-Ethoxycarbonylthieno[2,3-*b*]quinoxaline-3-sulfonylchloride	310	256.9	53.01
40	Ethyl 3-(*N*-methyl-*N*-phenyl)sulfamoylthieno[2,3-*b*]quinoxaline-2-carboxylate	180	93.55	86.44
41	3-(*N*-Methyl-*N*-phenyl)sulfamoylthieno[2,3-*b*]quinoxaline-2-carboxylic acid	220.5	228.2	−7.752
42	3-Amino-2-thieno[2,3-*b*]quinoxaline-2-carboxylic acid hydrazide	305.5	250.9	54.56
43	3-Amino-2-thieno[2,3-*b*]quinoxaline-2-carboazide	240	238.7	1.295
44	Imidazo[4′,5′:4,5]thieno[2,3-*b*]quinoxalin-2(1H,3H)-one	190	213.5	−23.55
45	3-Amino-pyrimido[4′,5′:4,5]thieno[2,3-*b*]quinoxalin-4(2H)-one	290	287.1	2.856
46	2-Amino-3-cyano-4-phenylpyridazino[2″,3″:1′,2′]pyrimido [4′,5′:4,5]thieno[2,3-*b*]quinoxalin-13-one	225	263.6	−38.66
47	3-(1-Pyrryl)pyrimido[4′,5′:4,5]thieno[2,3-*b*]quinoxalin-4(3H)-one	115	188.4	−73.48
48	3-Amino-2-(5-sulfanyl-1,3,4-oxadiazol-2-yl)thieno[2,3-*b*]quinoxaline	320	247.4	72.51
49	3-Amino-2-(5-hydrazino-1,3,4-oxadiazol-2-yl)thieno[2,3-*b*]quinoxaline	260	257.3	2.694
50	3-Amino-2-(3-sulfanyl-1,2,4-triazolo[3,4-*b*]oxadiazol-6-yl)thieno[2,3-*b*]quinoxaline	120	184	−64.08
51	3-Amino-2-(5-methylthio-1,3,4-oxadiazol-2-yl)thieno[2,3-*b*]quinoxaline	150	206.4	−56.43
52	3-Amino-2-(5-ethylacetatethio-1,3,4-oxadiazol-2-yl)thieno-[2,3-*b*]quinoxaline	240	225.4	14.54
53	2-Quinoxalinecarboxaldehyde hydrazone	145.5	188	−42.57
54	2-Quinoxalinecarboxaldehyde methylhydrazone	97	117.5	−20.56
55	2-Quinoxalinecarboxaldehyde benzylhydrazone	91.5	136.2	−44.7
56	2-Quinoxalinecarboxaldehyde phenylhydrazone	211	224.9	−13.9
57	2-Quinoxalinecarboxaldehyde *p*-tolylhydrazone	220.5	207.6	12.84
58	2-Quinoxalinecarboxaldehyde 4′-nitrophenylhydrazone	255.5	286.2	−30.71
59	2-Quinoxalinecarboxaldehyde 4′-carboxyphenylhydrazone	339	276.3	62.6
60	2-Quinoxalinecarboxaldehyde *N*,*N*-dimethylhydrazone	78.5	50.53	27.96
61	1-Methyl-1H-pyrazolo[3,4-*b*]quinoxaline	129.5	106	23.45
62	1-Benzyl-1H-pyrazolo[3,4-*b*]quinoxaline	113.5	69.69	43.8
63	2-Quinoxalinecarboxaldehyde oxime	195	205.6	−10.64
64	3-Benzyl-1H-quinoxalin-2-one	178.5	186.8	−8.319
65	3-Methyl-1H-quinoxalin-2-one	242	201.5	40.49
66	1,3-Dimethyl-1H-quinoxalin-2-one	76	140.1	−64.11
67	3-Benzyl-1-methyl-1H-quinoxalin-2-one	73	83.73	−10.73
68	1-Benzyl-3-methyl-1H-quinoxalin-2-one	90.5	117	−26.56
69	3-Bromomethyl-1H-1-methylquinoxalin-2-one	181	210.9	−29.93
70	3-(4-Cyanophenoxymethyl)-1-methyl-1H-quinoxalin-2-one	133	120	12.91
71	1-Methyl-3-(2,3,4,5,6-pentafluorophenoxymethyl)-1H-quinoxalin-2-one	129	129.3	−0.3363
72	3-(3,4-Dichlorophenoxymethyl)-1-methyl-1H-quinoxalin-2-one	106	128.8	−22.82
73	3-(4-Benzoylphenoxymethyl)-1-methyl-1H-quinoxalin-2-one	146	143.6	2.39
74	1-Methyl-3-(3-methyl-4-nitrophenoxymethyl)-1H-quinoxalin-2-one	141.5	202	−60.58
75	4-(4-Methyl-3-oxo-3,4-dihydroquinoxalin-2-ylmethoxy)-benzoic acid ethyl ester	152	117.8	34.12

[a] Diff.: difference between MP experimental and predicted.

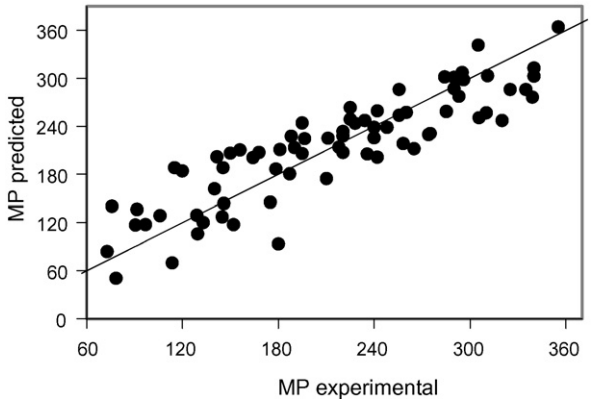

Fig. 2. Predicted vs. experimental MP.

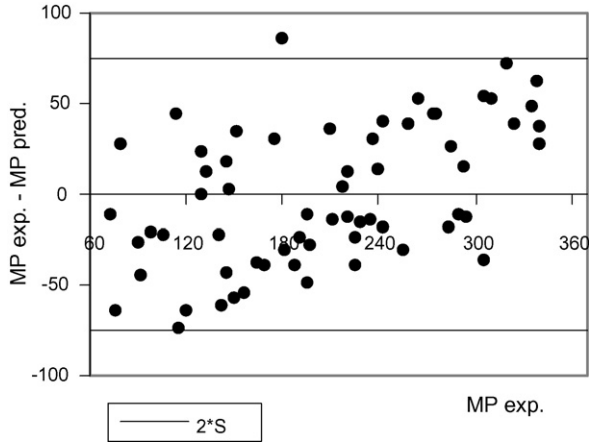

Fig. 3. Dispersion plot of the residuals for the model.

the model, measured as the maximum increase of S when removing each variable from Eq. (1), is ranked in the following way:

H-047 > Mor07u > nHDon > C-024 > XMOD > X3sol > Mor07p

The most important descriptor H-047 and the third ranked descriptor nHDon reveal the importance of hydrogens in influencing the MP, as they participate in intermolecular interactions through hydrogen bonds in the solid state. The second and seventh variables of this order, Mor07u and Mor07p, are molecular descriptor specially designed to reflect the distribution of an atomic property in the molecule; Mor07p expresses the distribution of atomic polarizabilities throughout all the structure, while Mor07u is the unweighted case, thus representing the distribution of the atoms in the molecule. Other descriptors are modified definitions of the Randic descriptors: XMOD and X3sol, reflecting the connectivity in the structure and the nature of atoms through quantum principal numbers.

4. Conclusions

Optimized geometries, harmonic vibrational frequencies, and ^{1}H chemical shifts were calculated for a family of 21 new quinoxaline derivatives using hybrid density functional theory. Selected dihedral angles, indicating the orientation of substituent groups with respect to the base quinoxaline moiety, were reported. No experimental information on geometrical parameters is available.

The calculated harmonic vibrational frequencies were considerably larger than the experimental values with absolute errors as large as 500 cm^{-1} for the NH group. A statistical analysis revealed that a scaling factor of about 0.92 diminishes the maximum error to about 200 cm^{-1}. The carbonyl group and other groups were better described by the level of theory used in this work.

The ^{1}H chemical shifts of those hydrogen atoms bound to carbon atoms were accurately described, but the corresponding ones to hydrogen atoms binding nitrogen and oxygen atoms were poorly described, with absolute errors of about 4 ppm.

As a next step, the MP of 75 quinoxaline derivatives were modeled by searching the optimal set of descriptors with the RM method among 875 theoretical molecular descriptors definitions, thus leading to a seven-parameter model whose predictions were satisfactory and possessed predictive ability.

In summary, the calculations carried out on a family of new quinoxalines with supposed biological activity would shed light into the preferred conformations shown by the molecules. Even though no biological processes were studied in the present work, the knowledge of the conformational preferences of a given molecule with biological activity is essential to understand how it could interact with a substrate.

Acknowledgements

R.P.D., E.A.C., and F.M.F. are members of the Scientific and Technological Researcher Career, CONICET, Argentina. P.R.D. and A.G.A. are fellows of CONICET. H.C. would like to thank Facultad de Ciencias Puras y Naturales, Universidad Mayor de San Andrés, La Paz-Bolivia.

Appendix A. Supplementary data

Supplementary data associated with this article can be found, in the online version, at doi:10.1016/j.jmgm.2006.03.004.

References

[1] S. Ceccarelli, A. D'Alessandro, M. Prinzivalli, S. Zanarella, Eur. J. Med. Chem. 33 (1998) 943.
[2] D. Catarzi, V. Colotta, F. Varano, L. Cecchi, G. Filacchioni, A. Galli, C. Costagli, J. Med. Chem. 42 (1999) 2478.
[3] O.S. Moustafa, M.S. Abbady, Afinidad 495 (2001) 335.
[4] HyperChem for Windows, Version 5.0, Hypercube, Inc., 1996.
[5] W. Kohn, L.J. Sham, Phys. Rev. 140 (1965) A1133.
[6] R.G. Parr, W. Yang, Density Functional Theory of Atoms and Molecules, Oxford University Press, 1989.
[7] A.D. Becke, J. Chem. Phys. 98 (1993) 5648.
[8] C. Lee, W. Yang, R.G. Parr, Phys. Rev. B 37 (1988) 785.
[9] J.M. Frisch, G.W. Trucks, H.B. Schlegel, G.E. Scuseria, M.A. Robb, J.R. Cheeseman, V.G. Zakrzewski, J.A. Montgomery Jr., R.E. Stratmann, J.C. Burant, S. Dapprich, J.M. Millam, A.D. Daniels, K.N. Kudin, M.C. Strain, O. Farkas, J. Tomasi, V. Barone, M. Cossi, R. Cammi, B. Mennucci, C. Pomelli, C. Adamo, C. Clifford, J. Ochterski, G.A. Petersson, P.Y. Ayala,

Q. Cui, K. Morokuma, D.K. Malick, A.D. Rabuck, K. Raghavachari, J.B. Foresman, J. Cioslowski, J.V. Ortiz, A.G. Baboul, B.B. Stefanov, G. Liu, A. Liashenko, P. Piskorz, I. Komaromi, R. Gomperts, R.L. Martin, D.J. Fox, T. Keith, M.A. Al-Laham, C.Y. Peng, A. Nanayakkara, C. Gonzalez, M. Challacombe, P.M.W. Gill, B. Johnson, W. Chen, M.W. Wong, J.L. Andres, C. Gonzalez, M. Head-Gordon, E.S. Replogle, J.A. Pople, Gaussian 98, Revision A.7, Gaussian, Inc., Pittsburgh, PA, 1998.

[10] J.R. Cheeseman, G.W. Trucks, T.A. Keith, M.J. Frisch, J. Chem. Phys. 104 (1996) 5497.

[11] Dragon Web, Version 3.0, http://www.disat.unimib.it/chm.

[12] P.R. Duchowicz, E.A. Castro, F.M. Fernández, M.P. González, Chem. Phys. Lett. 412 (2005) 376–380.

[13] P.R. Duchowicz, F.M. Fernández, E.A. Castro, MATCH Commun. Math. Comput. Chem. 55 (2006) 179–192.

[14] O.S. Moustafa, J. Chin. Chem. Soc. 47 (2) (2000) 351.

[15] O.S. Moustafa, M.Z.A. Badr, T.I. El-Emary, Bull. Korean Chem. Soc. 23 (4) (2002) 567.

[16] A.M. Boguslavskiy, M.G. Ponizovskiy, M.I. Kodess, V.N. Charushin, Russ. Chem. Bull. Int. Ed. 52 (10) (2003) 2175.

[17] D.S. Lawrence, J.E. Copper, C.D. Smith, J. Med. Chem. 44 (4) (2001) 594.